NEOPLASIA
www.neoplasia.com

Volume 23 Number xxx Month 2021 pp. 1078–1088

Cyst fluid metabolites distinguish malignant from benign pancreatic cysts ☆, ☆☆

Jiaqi Shi [a,*]; Zhujun Yi [a,b]; Lin Jin [a,b]; Lili Zhao [c]; Alexander Raskind [d]; Larisa Yeomans [e]; Zeribe C. Nwosu [f]; Diane M. Simeone [g]; Costas A. Lyssiotis [f]; Kathleen A. Stringer [e]; Richard S. Kwon [h]

[a] Department of Pathology & Clinical Labs, Rogel Cancer Center, University of Michigan, Ann Arbor, MI, USA
[b] Xiangya Hospital, Central South University, Changsha, Hunan, China
[c] Department of Biostatistics, University of Michigan, Ann Arbor, MI, USA
[d] Metabolomics Core, University of Michigan, Ann Arbor, MI, USA
[e] NMR Metabolomics Laboratory, Department of Clinical Pharmacy, College of Pharmacy, University of Michigan, Ann Arbor, MI, USA
[f] Department of Molecular & Integrative Physiology, Department of Internal Medicine, Division of Gastroenterology and Hepatology, Rogel Cancer Center, University of Michigan, Ann Arbor, MI, USA
[g] Perlmutter Cancer Center, NYU Langone Health, New York, NY, USA
[h] Internal Medicine, Michigan Medicine, Ann Arbor, MI, USA

Abstract

OBJECTIVES

Current standard of care imaging, cytology, or cystic fluid analysis cannot reliably differentiate malignant from benign pancreatic cystic neoplasms. This study sought to determine if the metabolic profile of cystic fluid could distinguish benign and malignant lesions, as well as mucinous and non-mucinous lesions.

Methods

Metabolic profiling by untargeted mass spectrometry and quantitative nuclear magnetic resonance was performed in 24 pancreatic cyst fluid from surgically resected samples with pathological diagnoses and clinicopathological correlation.

Results

(Iso)-butyrylcarnitine distinguished malignant from benign pancreatic cysts, with a diagnostic accuracy of 89%. (Iso)-butyrylcarnitine was 28-fold more abundant in malignant cyst fluid compared with benign cyst fluid (P=.048). Furthermore, 5-oxoproline (P=.01) differentiated mucinous from non-mucinous cysts with a diagnostic accuracy of 90%, better than glucose (82% accuracy), a previously described metabolite that distinguishes mucinous from non-mucinous cysts. Combined analysis of glucose and 5-oxoproline did not improve the diagnostic accuracy. In comparison, standard of care cyst fluid carcinoembryonic antigen (CEA) and cytology had a diagnostic accuracy of 40% and 60% respectively for mucinous cysts. (Iso)-butyrylcarnitine and 5-oxoproline correlated with cyst fluid CEA levels (P<.0001 and P<.05 respectively). For diagnosing malignant pancreatic cysts, the diagnostic accuracies of cyst size > 3 cm, ≥ 1 high-risk features, cyst fluid CEA, and cytology are 38%, 75%, 80%, and 75%, respectively.

* Corresponding author. Jiaqi Shi, Department of Pathology and Clinical Laboratories, University of Michigan, 2800 Plymouth Road, Building 35, Ann Arbor, MI 48109, USA.
E-mail addresses: jiaqis@umich.edu, jiaqis@med.umich.edu (J. Shi).

☆ Funding: This work is supported by the University of Michigan MCubed award, Michigan Regional Comprehensive Metabolomics Research Core Small Grant, and in part by National Cancer Institute (NCI) under award number K08CA234222 (to JS). CAL was supported by NCI under award numbers R37CA237421, R01CA248160, R01CA244931. This work utilized Core Services supported by grant DK097153 of NIH to the University of Michigan.
☆☆ Conflicts of interest: The authors state that they have no conflicts of interest.
Received 3 June 2021; received in revised form 1 September 2021; accepted 2 September 2021

https://doi.org/10.1016/j.neo.2021.09.004

Conclusions

(Iso)-butyrylcarnitine has potential clinical application for accurately distinguishing malignant from benign pancreatic cysts, and 5-oxoproline for distinguishing mucinous from non-mucinous cysts.

Neoplasia (2021) 23, 1078–1088

Keywords: Metabolite, Butyrylcarnitine, Diagnosis, Mucinous cyst, 5-oxoproline

Introduction

Early detection of pancreatic cancer is paramount because pancreatic cancer is the third leading cause of cancer death in the US [1]. Pancreatic cystic neoplasms, which are discovered with increasing frequency due to widespread use of imaging, represent the only currently detectable precursors to pancreatic cancer. The overall prevalence of incidental pancreatic cysts is up to 15% in adult patients compared to the approximately 0.008% incidence of pancreatic cancer [2–4]. An even higher prevalence is seen in age groups of 70 to 79 y of age (25%) and 80 y and over (37%). Pancreatic cystic neoplasms can be grouped into 2 categories: mucinous cysts and nonmucinous cysts. In general, mucinous cysts are considered as precursor lesions to adenocarcinoma, while nonmucinous cysts are mostly benign and have no malignant potential. However, the highest risk cysts are those mucinous cysts with high grade dysplasia or carcinoma (malignant cysts). Our ability to distinguish the cysts with the highest risk of malignant transformation remains inadequate using current standard diagnostic tools [5]. These inadequacies lead to either missed diagnosis of malignant cystic neoplasms, or unnecessary surveillance and surgeries, which can be associated with a 3.6% in-hospital mortality [6]. Therefore, there is an urgent need for new and more accurate diagnostic methods to identify cystic neoplasms with the highest risk of malignant transformation.

Current standard of care imaging or cyst fluid analysis cannot reliably differentiate malignant cyst from benign cystic lesions [5]. Cross-sectional imaging is usually the first test to identify these cystic lesions but has a limited ability to distinguish between the different cyst etiologies. High risk and worrisome imaging features include cyst size (≥3 cm), the presence of a mural nodule, thickened/enhancing cyst walls, main pancreatic duct dilation (≥5 mm), abrupt change in the caliber of the pancreatic duct with distal pancreatic atrophy, lymphadenopathy, increased serum CA 19-9, and cyst growth rate ≥5 mm/2 y according to the revised International Association of Pancreatology guidelines [7]. Given the relative lack of pathognomonic findings, the accuracy of imaging to determine the correct histologic diagnosis has been reported to range from 40% to 60% [8,9]. Cyst fluid biomarkers have been studied as well. Carcinoembryonic antigen (CEA) is the current biomarker of choice to differentiate mucinous from nonmucinous cysts with an accuracy of 79%; however, it cannot distinguish malignant from benign mucinous cysts [10]. Cytology has low sensitivity, ranging from 22% to 67%, to detect malignant cysts [11,12]. Although genomic and targeted sequencing and proteomics analysis have revealed some candidate genes and protein markers, none of these are widely accepted or clinically used [13–16]. Therefore, there is currently no routinely available clinical biomarker that accurately distinguishes malignant from benign cysts. This lack of accurate diagnostic biomarkers often leads to uncertainty in treatment options.

Altered metabolic pathways have recently been implicated in pancreatic cancer development [17–20]. So-called metabolic signatures have shown promise for several types of malignancies, including pancreatic cancer [17,21], but there is scarce data for pancreatic cystic neoplasms. Recent studies using semi-targeted metabolic profiling found 2 metabolites, glucose and kynurenine, that can distinguish mucinous from nonmucinous cysts, but they cannot distinguish malignant from benign cysts [22,23]. This semi-targeted derivation method labels only a subset of metabolites with certain chemical features [23].

In the current study, we used 2 different metabolomics analytical platforms (untargeted liquid chromatography-coupled mass spectrometry [LC-MS] and quantitative nuclear magnetic resonance [NMR]) to capture a broad range of different classes of metabolites. We aimed to identify new candidate metabolic biomarkers in cyst fluid to accurately distinguish malignant from benign cysts, in addition to mucinous from nonmucinous cysts.

Methods

Patient samples

Pancreatic cyst fluid samples (n = 24) were collected from consecutively resected pancreatic specimens of patients with cystic pancreatic neoplasms, including intraductal papillary mucinous neoplasm (IPMN, n = 11) and mucinous cystic neoplasm (MCN, n = 7), and nonmucinous cystic neoplasms (n = 6), including serous cystadenoma (SCA) and solid pseudopapillary neoplasm (SPN), from 2009 to 2016 at the University of Michigan (UM) Health System. The Institutional Review Board at the UM approved the study and informed consent was obtained from all study participants. The samples were divided into aliquots and stored at -80°C within 30 min of collection. Repeated freeze-thaw cycles were avoided for all samples. The diagnoses of all samples were confirmed by surgical pathology analysis. The electronic medical record was examined for clinical and demographic patient information.

Metabolic profiling

Untargeted metabolomics of pancreatic cyst fluid was performed using LC-MS (0.2 mL cyst fluid). Data were acquired on an Agilent Technologies 6530 Accurate-Mass Quadrupole Time-of-Flight instrument with dual Agilent Jet Stream electrospray ionization at the Michigan Regional Comprehensive Metabolomics Resource Core facility at the UM. Samples were processed and analyzed according to the core's standard protocols. Please refer to the Supplementary Materials for detailed description. Appropriate quality controls were carried out. Two complementary data sets were generated from the same samples—1 in positive mass spectrometry mode and another in negative mode. The use of both positive and negative ionization provided more comprehensive metabolome coverage than single polarity [24]. Raw data processing was done using Agilent software (MassHunter Qual and ProFinder). Data analysis was performed with Agilent MassProfiler Pro package using recursive analysis workflow.

NMR (0.5 mL cyst fluid) spectra were acquired at the UM's Biochemical NMR Core Laboratory on an Agilent, 500 MHz NMR spectrometer with a VNMRS console operated by host software VNMRJ 4.0 and equipped with a 5mm One-Probe. Spectra were recorded twice for each sample. First, 128 scans were acquired to ascertain the amount of internal standard required. The Chenomx internal standard, DSS-d_6 (3-(Trimethylsilyl)-1-propanesulfonic acid-d_6 sodium salt, 0.1-0.5 mM), was used as a reference signal for the quantification of metabolites. After the addition of the internal standard, 1,024 scans were collected. Each spectrum was acquired at 25°C using the first increment of the standard NOESY (nuclear Overhauser effect spectroscopy) pulse sequence as previously described [25]. The resulting NMR spectra were analyzed using Chenomx Suite 8.1 (Chenomx, Inc.). The Processor module was used to phase shift and baseline correct each spectrum. Compounds were then identified and quantified in the Profiler module of the software, which accounted for the pH of the sample and the concentration of the internal standard and quantified metabolite concentration relative to the internal standard. Metabolite identity was confirmed using the Chenomx Compound Library, which contains 338 compounds.

Statistical analysis

Wilcoxon Rank-Sum tests were used to compare metabolites between different groups. Fisher's exact test was used to validate the accuracy of the metabolites to distinguish malignant from benign cysts or mucinous from nonmucinous cysts. The obtained P values were further adjusted for multiple hypothesis correction using Benjamini-Hochberg procedure [26]. For each significant metabolite, the receiver operating characteristic (ROC) curve was plotted and area under the curve (AUC) was calculated to assess the predictive accuracy of that metabolite. Relationship of these metabolites with each other and other clinical features and patient prognostic factors was evaluated using Spearman Correlation Coefficient test or Wilcoxon Rank Sum test. Overall and progression-free survival (OS and PFS) curves were estimated using Kaplan-Meier methods and compared using log-rank tests. Significance is determined if $P < 0.05$. These analyses were conducted using SAS (version 9.4, SAS Institute, Cary, NC). Visualization of metabolite data in heat map was performed with R statistical programming software (version 3.5.2). Metabolites with no ion count data in more than half of the samples were excluded. The data points of the remaining metabolites were then log2-transformed and plotted using the package gplots (version 3.0.1).

Results

Clinical features of pancreatic cysts correlate with diagnostic accuracy and survival outcome

We will focus on 21 pancreatic cyst fluid samples that were analyzed by both NMR and LC-MS. Another 3 samples were only analyzed by NMR. Cyst fluid was profiled from patients with the following clinical characteristics. Eight patients had Whipple procedure, 1 had total pancreatectomy, and twelve had distal pancreatectomy. Ten patients were symptomatic at the time of diagnosis and 11 patients were asymptomatic. Clinical and imaging features of the pancreatic cysts for metabolomic analysis are summarized in Table 1. Fifteen of the cysts were mucinous cysts and 6 were nonmucinous cysts. Mucinous cysts included IPMN (n = 8) and MCN (n = 7), and nonmucinous cysts included SCA (n = 5) and SPN (n = 1). Malignant mucinous cysts included IPMNs with either high-grade dysplasia or invasive adenocarcinoma (n = 3). All 21 pancreatic cysts had final surgical pathology, radiology, and clinical presentation information available. Of the 21 pancreatic cysts, 10 also had endoscopic ultrasound guided fine needle aspiration and cytology performed, 15 had serum CA19.9 measured, and 5 had cyst fluid CEA measured.

There was a female predominance in both mucinous (female:male = 3) and nonmucinous cysts (female:male = 5) due to the nature of the pancreatic cystic neoplasms, i.e., MCN, SCA, and SPN, which predominantly occur in women (Table 1). Cytology was the only parameter that was significantly different between mucinous and nonmucinous cysts ($P = 0.048$). Two of the 6 (33%) mucinous cysts had suspicious or positive for neoplastic cell cytology, while all 4 (100%) nonmucinous cysts had negative cytology. However, the overall diagnostic sensitivity, specificity, and accuracy of cytology for diagnosing mucinous cysts were 33%, 100%, and 60% respectively. There were no statistical differences in age, sex, cyst size, cyst location, high-risk features (main duct dilation, mural nodule, pancreatitis, jaundice), cyst fluid CEA, or serum CA19-9 between mucinous and nonmucinous cysts. Cyst fluid CEA was only elevated above 192 ng/mL in 2 of the 5 mucinous cysts (a diagnostic sensitivity and accuracy of 40%) [27]. For diagnosing malignant pancreatic cysts, the diagnostic accuracies of cyst size >3 cm, ≥1 high-risk features, cyst fluid CEA, or cytology are 38%, 75%, 80%, 75% respectively. Interestingly, pancreatitis (present in 3/21 patients) was the only clinical factor that significantly impacted both OS and PFS ($P < 0.05$, Fig. 1).

Untargeted metabolomics profiling reveals predictive metabolites

A total of 360 and 212 metabolites were identified in the positive and negative modes, respectively, in at least 1 sample (Supplementary Table 1). Fourteen metabolites were significantly different between mucinous and nonmucinous cysts and 15 metabolites were significantly different between malignant and benign mucinous cysts ($P < 0.05$) (Table 2). In addition, multiple metabolites were different between malignant and benign IPMNs, IPMN and MCN, IPMN and nonmucinous cysts, and MCN and nonmucinous cysts (Table 2).

Among the 14 metabolites that were significantly different between mucinous and nonmucinous cysts ($P < 0.05$), 9 metabolites were identified by positive mode MS and 6 by negative mode MS (Table 3). We identified 5-oxoproline and isocitric acid as the top 2 metabolites that differentiated mucinous from nonmucinous cysts, with 5-oxoproline having the lowest P value. As a proof of concept, glucose, but not kynurenine, also differentiated mucinous from nonmucinous cysts, as previously described [23]. The ion count of 5-oxoproline was 5-fold higher in nonmucinous than mucinous cyst fluid. There is no overlap of the range of 5-oxoproline ion count between mucinous and nonmucinous cysts. Furthermore, the diagnostic accuracy (AUC) of 5-oxoproline detected by positive mode is 0.9 (90% accuracy), comparing to the AUC of glucose of 0.82 (Fig. 2A). A heat map of 5-oxoproline showed a distinct profile between nonmucinous and mucinous cysts compared to glucose (Fig. 2B). Additionally, the combination of glucose and 5-oxoproline did not improve the diagnostic accuracy.

Among the 15 metabolites that were significantly different between malignant and benign mucinous cysts, 10 metabolites were identified by positive mode MS and 7 by negative mode MS (Table 4). Theophylline and hippuric acid were identified by both positive and negative mode MS. However, only the ion counts of 2 metabolites out of the 15 butyrylcarnitine and iso-butyrylcarnitine were distinct between mucinous and nonmucinous cysts. While the other 13 metabolites can distinguish malignant and benign mucinous cysts, they cannot distinguish mucinous from nonmucinous cysts. Since butyrylcarnitine and iso-butyrylcarnitine are not well-separated by MS, we reported them here as a mixture labelled as (iso)-butyrylcarnitine. (Iso)-butyrylcarnitine was 28-fold more abundant in malignant cyst fluid compared with benign cyst fluid ($P = 0.048$). Representative ROC curves showing the AUCs (diagnostic accuracies) of (iso)-butyrylcarnitine comparing to glucose AUC to distinguish malignant from benign cysts, including nonmucinous cysts, is illustrated in Fig. 3A. (Iso)-Butyrylcarnitine had an AUC of 0.89, much more accurate than glucose (0.65). This result is consistent with previous observation that glucose cannot distinguish malignant from benign pancreatic cysts [23]. Heat maps of ion

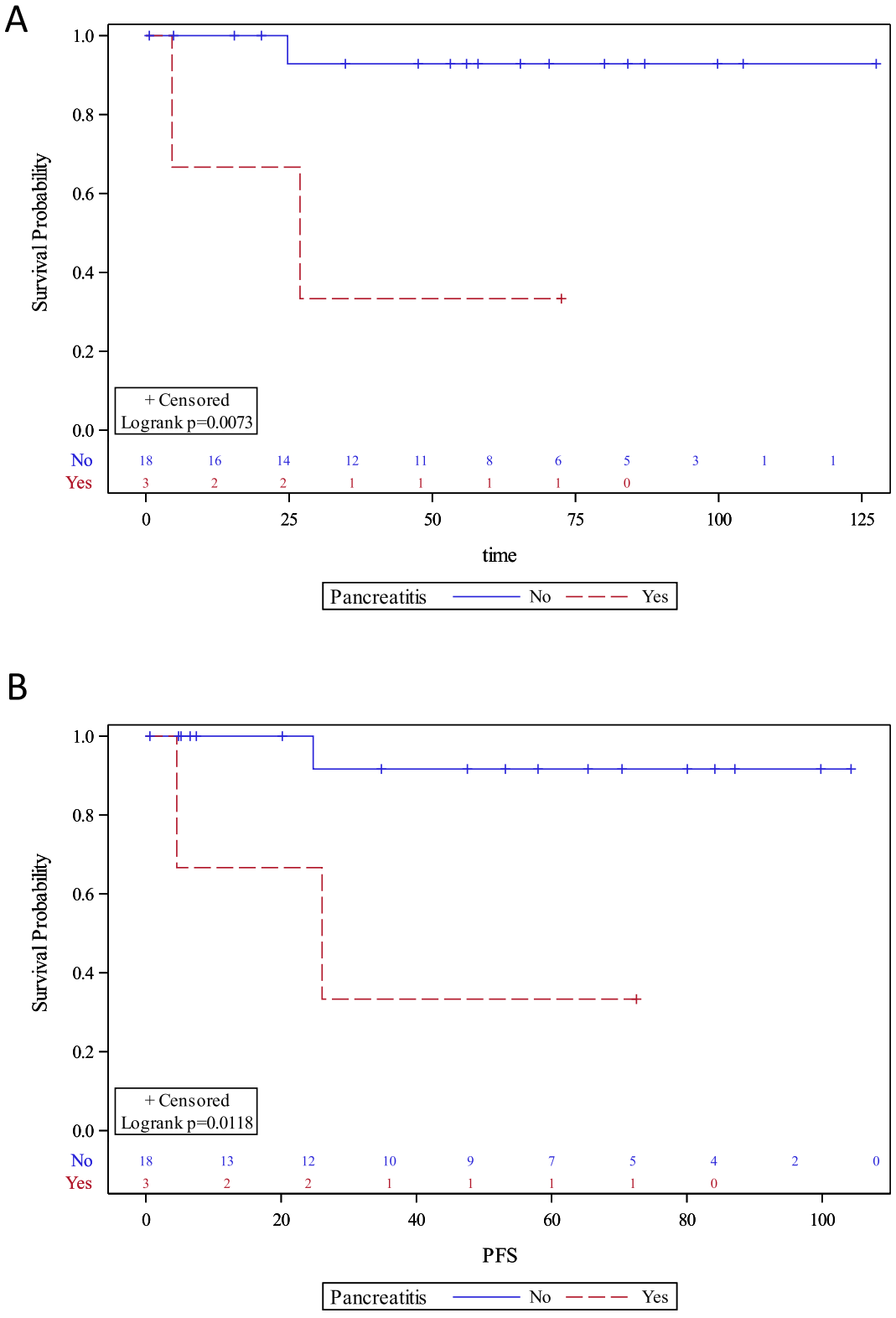

Fig. 1. Kaplan-Meier curves of (A) overall survival and (B) progression-free survival (PFS) of pancreatic cyst patients with or without pancreatitis.

Table 1

Clinical features of pancreatic cysts.

	Mucinous Cyst(n = 15)	Nonmucinous Cyst (n = 6)	*P* Value
Female:male (ratio)	11:4 (3)	5:1 (5)	1.00
Mean age (range)	57.6 (32−74)	56.3 (36−78)	1.00
Cyst size, mean (range), cm	5.8 (2.4−10.9)	6.1 (3−10.7)	0.28
Cyst location			1.00
Head/neck, n/n (%)	6/15 (40)	3/6 (50)	
Body/tail, n/n (%)	9/15 (60)	3/6 (50)	
High-risk features, n/n (%)	7/15 (47)	2/6 (33)	
Main duct dilation	4/15 (27)	1/6 (17)	1.00
Mural nodule	5/15 (33)	1/6 (17)	0.62
Pancreatitis	3/15 (20)	0/6 (0)	0.53
Jaundice	0/15 (0)	1/6 (17)	0.29
Cyst fluid CEA, mean (range), ng/mL	104619 (141−522000)	NP	N/A
Serum CA19.9, mean (range), U/mL	34 (2−125)	30 (3−73)	1.00
Cytology, n/n (%)	n = 6	n = 4	**0.048**
Negative,	1/6 (17)	4/4 (100)	
Atypical	3/6 (50)	0/4 (0)	
Suspicious	1/6 (17)	0/4 (0)	
Positive	1/6 (17)	0/4 (0)	
Final surgical pathology	n = 15	n = 6	N/A
IPMN, n/n (%)	8/15 (53)	N/A	
LGD	5/15 (33)	N/A	
HGD/CA	3/15 (20)	N/A	
MCN with LGD, n/n (%)	7/15 (47)	N/A	
SCA, n/n (%)	N/A	5/6 (83)	
SPN, n/n (%)	N/A	1/6 (17)	

CA = cancer; HGD = high-grade dysplasia; IPMN = intraductal papillary mucinous neoplasm; LGD = low-grade dysplasia; MCN = mucinous cystic neoplasm; N/A = not applicable; NP = not performed; SCA = serous cystadenoma; SPN = solid pseudopapillary neoplasm. Bold: $P<0.05$.

Table 2

Number of metabolites identified by MS and NMR that were different between various pancreatic cystic neoplasms ($P < 0.05$).

Differential Diagnosis	Metabolites by MS(n = 21)	Metabolites by NMR (n = 24)
Mucinous vs nonmucinous	14	8
Malignant vs benign mucinous	15	2
Malignant vs benign IPMN	8	1
IPMN vs nonmucinous	11	12
MCN vs nonmucinous	17	1
IPMN vs MCN	4	1

IPMN = intraductal papillary mucinous neoplasm; MCN = mucinous cystic neoplasm; MS = mass spectrometry; NMR = nuclear magnetic resonance.

counts of (iso)-butyrylcarnitine and glucose were shown in Fig. 3B, which highlighted the distinct (iso)-butyrylcarnitine measurement patterns between benign and malignant cysts. A heat map demonstrating the metabolic profile of malignant and benign mucinous and benign nonmucinous pancreatic cyst fluid samples were shown in Fig. 4 with (iso)-butyrylcarnitine, 5-oxoproline, and glucose highlighted.

We then sought to investigate the relationships of (iso)-butyrylcarnitine, 5-oxoproline, and glucose with each other and other clinical features and patient prognostic factors, such as cyst fluid CEA, cyst size, high risk imaging findings including mural nodule and main pancreatic duct dilation. The levels of 5-oxoproline and glucose were significantly correlated with each other ($R^2 = 0.4142$, $P < 0.0001$, Fig. 5A). However, there was no correlation between (iso)-butyrylcarnitine and 5-oxoproline, and (iso)-butyrylcarnitine and glucose. There were correlations between fluid CEA and (iso)-butyrylcarnitine, 5-oxoproline, and glucose (Fig. 5B−D). However, there was no correlation between (iso)-butyrylcarnitine, 5-oxoproline, and glucose, and cyst size, imaging findings of mural nodule or main pancreatic duct dilation.

Nuclear magnetic resonance metabolomics

A total of 41 metabolites were identified in at least 1 pancreatic cyst fluid sample (Supplementary Table 2). Eight metabolites were significantly different between mucinous and nonmucinous cysts and 2 metabolites were

Table 3

Metabolites identified by MS that were different between mucinous and nonmucinous pancreatic cysts ($P < 0.05$).

Metabolites	Mucinous (n = 15) Median (IQR), ion Count	Nonmucinous (n = 6) Median (IQR), ion Count	*P* Value
Positive mode			
5-OXOPROLINE	**328291 (96091–485158)**	**1518087 (1364086–2789189)**	**0.010**
GLUCOSE	128524 (56747–703095)	1370490 (1025144–1426303)	0.012
4-HYDROXY-L-PROLINE	35788 (27030–78656)	101112 (97957–175758)	0.013
N-ACETYL-DL-SERINE	324436 (75648–342125)	1454784.5 (1234557–2525428)	0.018
3-METHOXYTYROSINE	14833 (14301–29458)	46125 (41753–51654)	0.024
CYSTATHIONINE	3151 (2633–7181)	17203.5 (13938–17747)	0.024
TRANS-4-HYDROXYPROLINE	35788 (25365–84012)	101112 (97957–175758)	0.029
5-AMINOLEVULINIC ACID	35788 (25365–84012)	138435 (100323–181980)	0.034
CORTICOSTERONE	5504 (2721–6985)	13526 (8740–18319)	0.034
Negative mode			
ISOCITRIC ACID	116309 (76235–159209)	335226 (221004–473141)	0.006
5-OXOPROLINE	**305488 (70769–446892)**	**1880533.5 (1416588–3323930)**	**0.006**
CORTISOL	20914 (10350–27580)	46029 (33656–75199)	0.023
MYRISTIC ACID	88555 (85362–118834)	127643 (122344–157801)	0.023
LAURIC ACID	11764 (8593–16257)	18380.5 (14613–39039)	0.037
PHYTANIC ACID	4687.5 (3817–6835)	12446.5 (9643–14340)	0.041

IQR = interquartile range; MS = mass spectrometry. Bold: metabolite with the lowest *P* value in both positive and negative mode without overlap of the range of ion count values between mucinous and non-mucinous cysts.

Table 4

Metabolites identified by MS that were different between malignant and benign pancreatic mucinous cysts ($P < 0.05$).

Metabolites	Benign Mucinous (n = 12)Median (IQR), ion Count	Malignant Mucinous (n = 3)Median (IQR), ion Count	*P* Value
Positive mode			
HYPOXANTHINE	181015 (62556–758910)	1908260 (1818216–4220855)	0.007
THEOPHYLLINE	26958 (11475–36585)	92666 (74052–98871)	0.013
CITRIC ACID	91736 (52944–144816)	337347 (279832–378039)	0.018
CAFFEINE	621768 (117339–943485)	2656266 (2073044–3239489)	0.026
ASCORBIC ACID	164495 (25951–261638)	373623 (364225–678897)	0.028
BUTYRYLCARNITINE	**42559 (20645–290513)**	**1184524 (675297–1535337)**	**0.048**
ISO-BUTYRYLCARNITINE	**42559 (20645–290549)**	**1182716 (674253–1533280)**	**0.048**
URIC ACID	701262.5 (228542–1694508)	2540869 (2469800–2610931)	0.031
3-HYDROXYBENZALDEHYDE	34440 (13578–64573)	159965 (130737–182655)	0.036
HIPPURIC ACID	80276 (25637–187719)	329828 (269379–383050)	0.036
Negative mode			
THEOPHYLLINE	55952 (28465–98926)	282772 (223165–301222)	0.007
SUCCINIC ACID	82669.5 (55772–212891)	395809 (339282–744334)	0.031
1-METHYLXANTHINE	28466 (17629–50712)	131689 (97207–190481)	0.033
4-ACETAMINOPHEN	125170 (26805–156488)	3637571 (3199494–3664005)	0.036
SULFATE			
16:0 LYSO PC	18142.5 (10487–74808)	2929.5 (2253–3606)	0.044
HIPPURIC ACID	132079 (36813–267969)	499781 (404656–581239)	0.049
INOSINE	52133 (6037–112142)	166121 (143710–510274)	0.049

IQR = interquartile range; MS = mass spectrometry.

significantly different between malignant and benign mucinous cysts ($P < 0.05$) (Table 2). In addition, multiple metabolites were different between malignant and benign IPMNs, IPMN and MCN, IPMN and nonmucinous cysts, and MCN and nonmucinous cysts.

The 8 metabolites that were significantly different between mucinous and nonmucinous cysts are shown in Table 5. Table 6 showed the 2 metabolites (ornithine and glutamate) that are also different between malignant and benign mucinous cysts. However, values of both ornithine and glutamate from malignant mucinous cyst fluid overlapped with those from nonmucinous cyst fluid. Therefore, ornithine and glutamate are not suitable to distinguish malignant mucinous cysts from benign nonmucinous cysts.

Discussion

In this study, we report that (iso)-butyrylcarnitine can distinguish malignant from benign pancreatic cysts with 89% diagnostic accuracy.

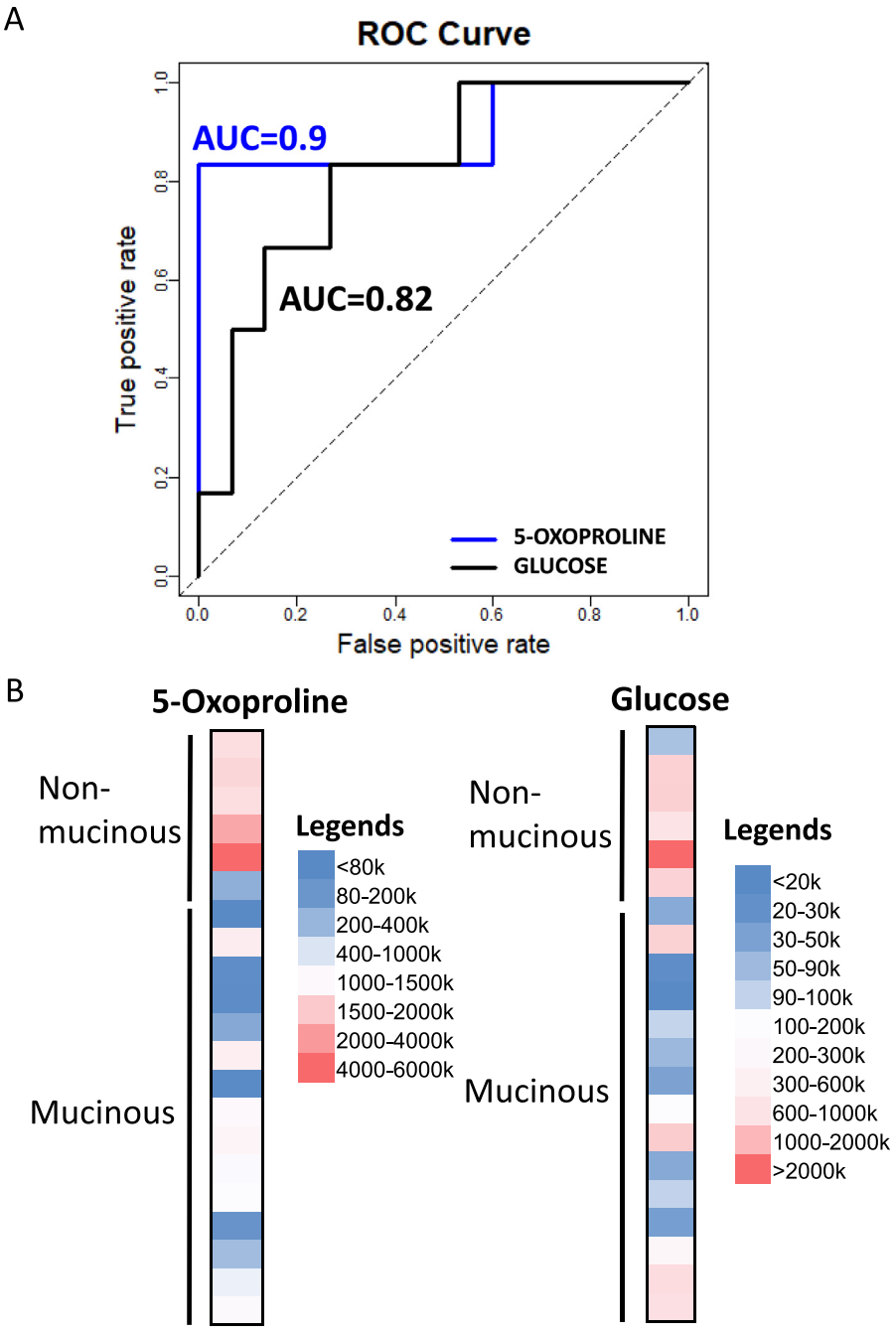

Fig. 2. (A) ROC curves of 5-oxoproline and glucose differentiating mucinous from nonmucinous cysts using LC-MS. AUC, area under the curve; LC-MS, liquid chromatography-coupled mass spectrometry; ROC, receiver operating characteristic. (B) Representative heat maps of 5-oxoproline and glucose MS ion counts comparing nonmucinous and mucinous pancreatic cysts.

We also identified 5-oxoproline as a candidate diagnostic marker for distinguishing mucinous from nonmucinous pancreatic cysts with 90% diagnostic accuracies. Validation of these candidate biomarkers in a larger, more diverse cohort of patients will be an important next step to confirm their predictive value.

Compared to other metabolomics studies, our study has several unique characteristics. First, we utilized pancreatic cyst fluid, a specimen that can be routinely obtained in clinical diagnostic setting. Identification of metabolic biomarkers in serum has achieved limited, if any, success. This is due to the many confounding factors, such as diet and complex metabolic pattern of serum [23]. Second, we used a broad metabolomics approach, which improves the capture of a greater number of metabolites, compared to more targeted approaches [22,23,28]. Third, we included less common, but important, pancreatic cystic neoplasms (MCN and SPN) samples. Therefore, our samples cover a wider variety of pancreatic cysts that can be encountered clinically compared to a few recent cyst fluid metabolomics studies which only included IPMN and SCA samples [28,29].

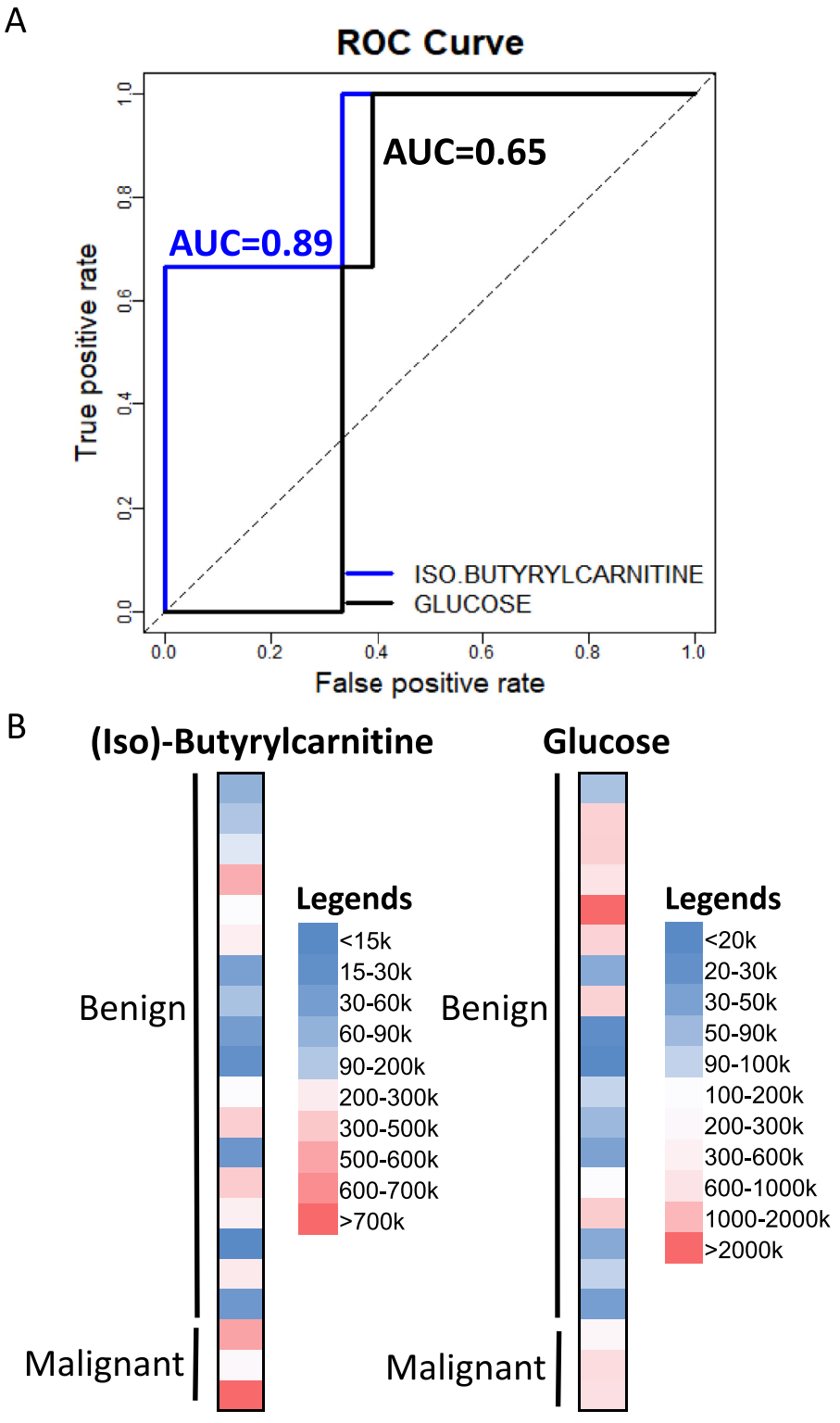

Fig. 3. (A) ROC curves of (iso)-butyrylcarnitine and glucose differentiating malignant from benign cysts using LC-MS. AUC, area under the curve; LC-MS, liquid chromatography-coupled mass spectrometry; ROC, receiver operating characteristic. (B) Representative heat maps of (iso)-butyrylcarnitine and glucose MS ion counts comparing benign and malignant pancreatic cysts.

Table 5

Metabolites identified by NMR that were different between mucinous and nonmucinous pancreatic cysts ($P < 0.05$).

Metabolites	Mucinous (n = 18) Median (IQR), μM	Nonmucinous (n = 6) Median (IQR), μM	*P* value
Acetate	18.8 (15.8–28.6)	43.5 (40.2–47.6)	0.005
Valine	36.95 (5.8–153)	230 (147.3–296.6)	0.025
Creatine	26.2 (16.7–44)	57.55 (49.5–65.2)	0.029
Methionine	0 (0–16.4)	36.55(31.1–41.9)	0.036
Ornithine	0 (0–37.3)	145.2 (86.2–155.9)	0.044
Glucose	392.5 (132.3–3205.2)	4549.75 (2340.6–5716.1)	0.045
Glutamate	0 (0–69)	226.4 (127.3–236.3)	0.045
Isoleucine	16.15 (0–52.3)	73 (49–77.6)	0.049

IQR = interquartile range; NMR = nuclear magnetic resonance.

Table 6

Metabolites identified by NMR that were different between malignant and benign pancreatic mucinous cysts ($P < 0.05$).

Metabolites	Benign Mucinous (n = 14) Median (IQR), μM	Malignant Mucinous (n = 4) Median (IQR), μM	*P* Value
Ornithine	0 (0–0)	45.3 (34.4–56.7)	0.018
Glutamate	0 (0–0)	144.1 (143.3–163.5)	0.024

IQR = interquartile range; NMR = nuclear magnetic resonance.

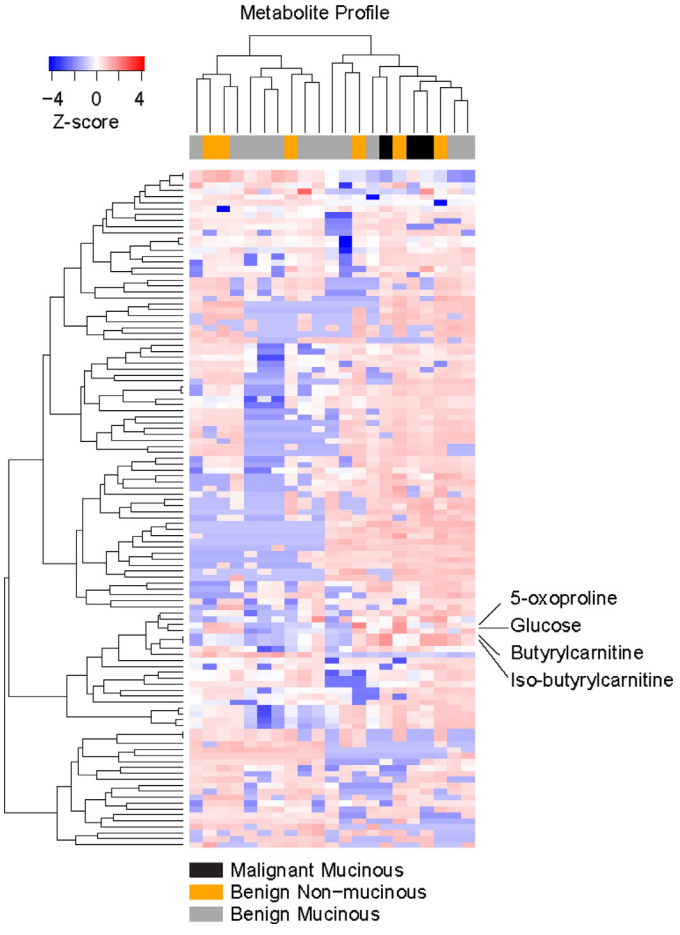

Fig. 4. A heat map showing metabolic profile of mucinous and nonmucinous pancreatic cyst fluid samples. Legend indicates z-score denoting the relative abundance of the metabolites.

Similar to previous studies, we also identified glucose as one of the metabolites that is significantly different between mucinous and nonmucinous cysts [22,23]. However, its diagnostic accuracy of 82% is inferior to 5-oxoproline (90% accuracy). Addition of glucose to 5-oxoproline did not improve the diagnostic accuracy of 5-oxoproline. Our data also confirmed that glucose cannot distinguish malignant from benign cysts. In addition, we did not identify kynurenine as a candidate biomarker to differentiate mucinous from nonmucinous cysts in our cyst fluid samples, which could be a result of our limited sample size.

Butyrylcarnitine and iso-butyrylcarnitine are members of the compound class known as acylcarnitines. They are elevated in patients with the deficiency of short-chain acyl-CoA dehydrogenase (ACAD), which is a mitochondrial enzyme that catalyzes the initial step of the fatty acid beta-oxidation pathway, and can be detected in blood and urine [30–32]. Interestingly, butyrylcarnitine and iso-butyrylcarnitine are markedly elevated in most malignant pancreatic cysts compared to benign cysts. The etiology of this elevation is unclear. However, short-chain ACAD expression is downregulated in hepatocellular carcinoma which promotes cancer cell proliferation and metastasis [33]. Other family members of ACAD have been implicated in regulating pancreatic cancer cell viability and immune cells in the tumor microenvironment [34,35]. Upregulation of ACAD family member-10 is required for metformin to kill pancreatic cancer cells. Intrapancreatic CD8+ T cells downregulate the very-long-chain ACAD which lead to accumulation of fatty acids and lipotoxicity in T cells.

Although our data are promising, there are limitations. These include the small sample size and the retrospective nature of the study. Additionally, this study did not include other less common types of pancreatic cysts, such as cystic neuroendocrine tumors. We also only included patients with a definitive histologic diagnosis who underwent surgery, which could introduce a selection bias. Prospective larger cohort studies are needed to validate these candidate biomarkers.

In conclusion, we used a broad metabolic profiling approach on a small cohort of histologically defined pancreatic cysts. We discovered that (iso)-butyrylcarnitine and 5-oxoproline show promising diagnostic accuracy distinguishing malignant from benign pancreatic cysts and mucinous from

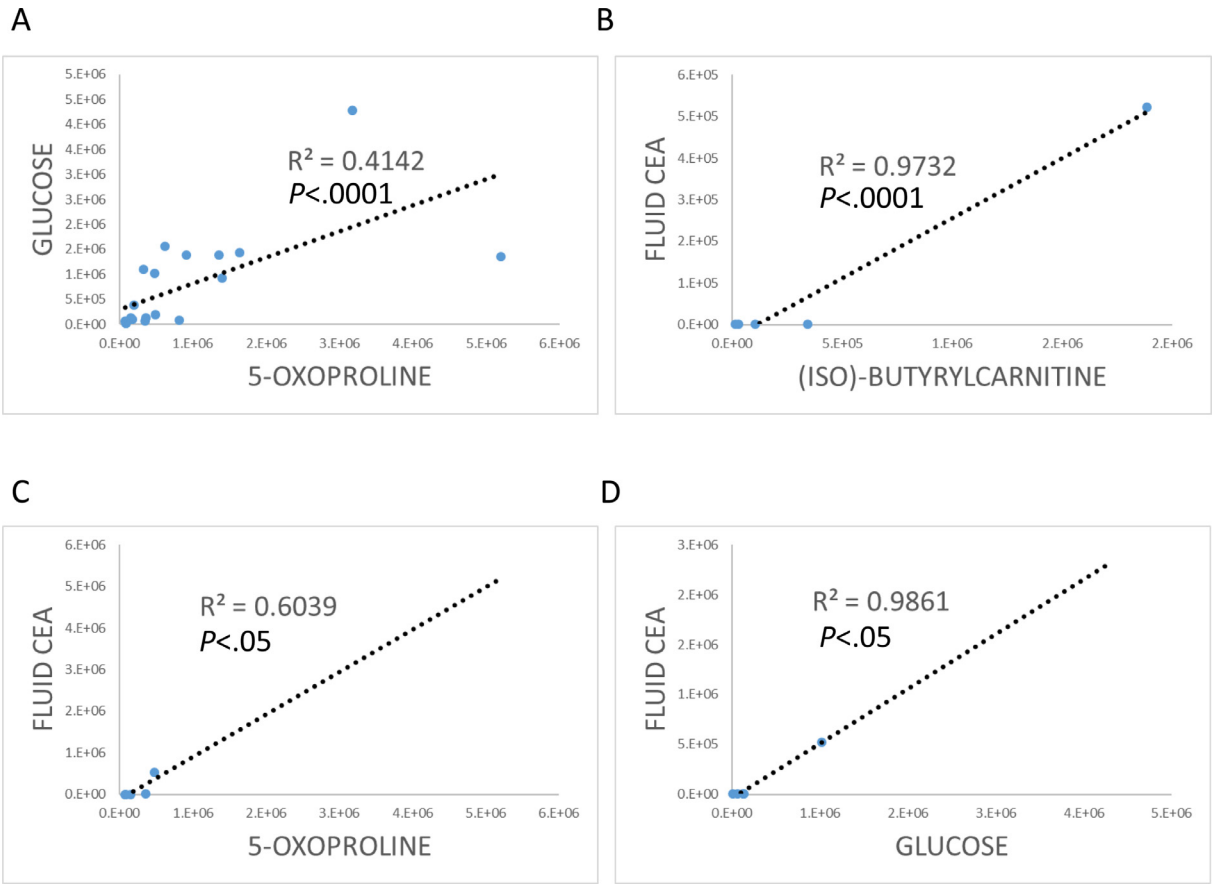

Fig. 5. Scatter charts showing relationships between (A) 5-oxoproline and glucose, fluid CEA (ng/mL) and (B) (iso)-butyrylcarnitine, (C) 5-oxoproline, or (D) glucose.

nonmucinous pancreatic cysts. Upon clinical validation, these biomarkers may contribute to patients' clinical care with pancreatic cysts, namely the accurate diagnosis and early detection of cancer, prevention of malignant transformation, and guidance of clinical treatment decision making.

Acknowledgments

We thank the NMR Metabolomics Laboratory and the Biochemical Nuclear Magnetic Resonance Core, College of Pharmacy, and the Michigan Regional Comprehensive Metabolomics Resource Core at University of Michigan for performing the NMR and LC-MS data acquisition.

Author contributions

Study design, data acquisition, data analysis, and manuscript preparation: Jiaqi Shi; sample collection and storage: Zhujun Yi and Lin Jin; data analysis and manuscript preparation: Lili Zhao, Zeribe C. Nwosu; data acquisition and analysis: Alexander Raskind and Larisa Yeomans; provision of samples: Diane Simeone; study design: Richard Kwon, Costas Lyssiotis, and Kathleen Stringer.

Supplementary materials

Supplementary material associated with this article can be found, in the online version, at doi:10.1016/j.neo.2021.09.004.

References

1 Rahib L, Smith BD, Aizenberg R, Rosenzweig AB, Fleshman JM, Matrisian LM. Projecting cancer incidence and deaths to 2030: the unexpected burden of thyroid, liver, and pancreas cancers in the United States. *Cancer Res* 2014;**74**:2913–21.

2 Farrell JJ. Prevalence, diagnosis and management of pancreatic cystic neoplasms: current status and future directions. *Gut Liver* 2015;**9**:571–89.

3 Lee KS, Sekhar A, Rofsky NM, Pedrosa I. Prevalence of incidental pancreatic cysts in the adult population on MR imaging. *Am J Gastroenterol* 2010;**105**:2079–84.

4 Rawla P, Sunkara T, Gaduputi V. Epidemiology of pancreatic cancer: global trends, etiology and risk factors. *World J Oncol* 2019;**10**:10–27.

5 Stark A, Donahue TR, Reber HA, Hines OJ. Pancreatic cyst disease: a review. *JAMA* 2016;**315**:1882–93.

6 van Rijssen LB, Koerkamp BG, Zwart MJ, Bonsing BA, Bosscha K, van Dam RM, van Eijck CH, Gerhards MF, van der Harst E, de Hingh IH, et al. Nationwide prospective audit of pancreatic surgery: design, accuracy, and outcomes of the Dutch Pancreatic Cancer Audit. *HPB (Oxford)* 2017;**19**:919–26.

7 Tanaka M, Fernandez-Del Castillo C, Kamisawa T, Jang JY, Levy P, Ohtsuka T, Salvia R, Shimizu Y, Tada M, Wolfgang CL. Revisions of international consensus Fukuoka guidelines for the management of IPMN of the pancreas. *Pancreatology* 2017;**17**:738–53.

8 Visser BC, Yeh BM, Qayyum A, Way LW, McCulloch CE, Coakley FV. Characterization of cystic pancreatic masses: relative accuracy of CT and MRI. *AJR Am J Roentgenol* 2007;**189**:648–56.

9 Fisher WE, Hodges SE, Yagnik V, Moron FE, Wu MF, Hilsenbeck SG, Raijman IL, Brunicardi FC. Accuracy of CT in predicting malignant potential of cystic pancreatic neoplasms. *HPB (Oxford)* 2008;**10**:483–90.

10 Brugge WR, Lewandrowski K, Lee-Lewandrowski E, Centeno BA, Szydlo T, Regan S, del Castillo CF, Warshaw AL. Diagnosis of pancreatic cystic neoplasms: a report of the cooperative pancreatic cyst study. *Gastroenterology* 2004;**126**:1330–6.

11 Heidarian A, Das KK, Mino-Kenudson M, Fernandez-Del Castillo C, Pitman MB. Cytology adds value to monoclonal antibody Das-1 testing for detection of high-risk pancreatic cysts. *J Am Soc Cytopathol* 2021;**10**(3):249–54.

12 Estrada P, Benson M, Gopal D, Buehler D, Pfau P. Cytology with rapid on-site examination (ROSE) does not improve diagnostic yield of EUS-FNA of pancreatic cystic lesions. *Diagn Cytopathol* 2019;**47**:1184–9.

13 Singhi AD, McGrath K, Brand RE, Khalid A, Zeh HJ, Chennat JS, Fasanella KE, Papachristou GI, Slivka A, Bartlett DL, et al. Preoperative next-generation sequencing of pancreatic cyst fluid is highly accurate in cyst classification and detection of advanced neoplasia. *Gut* 2018;**67**:2131–41.

14 Khalid A, Zahid M, Finkelstein SD, LeBlanc JK, Kaushik N, Ahmad N, Brugge WR, Edmundowicz SA, Hawes RH, McGrath KM. Pancreatic cyst fluid DNA analysis in evaluating pancreatic cysts: a report of the PANDA study. *Gastrointest Endosc* 2009;**69**:1095–102.

15 Wu J, Matthaei H, Maitra A, Dal Molin M, Wood LD, Eshleman JR, Goggins M, Canto MI, Schulick RD, Edil BH, et al. Recurrent GNAS mutations define an unexpected pathway for pancreatic cyst development. *Sci Transl Med* 2011;**3**:92ra66.

16 Al Efishat MA, Attiyeh MA, Eaton AA, Gonen M, Prosser D, Lokshin AE, Castillo CF, Lillemoe KD, Ferrone CR, Pergolini I, et al. Multi-institutional validation study of pancreatic cyst fluid protein analysis for prediction of high-risk intraductal papillary mucinous neoplasms of the pancreas. *Ann Surg* 2018;**268**:340–7.

17 Son J, Lyssiotis CA, Ying H, Wang X, Hua S, Ligorio M, Perera RM, Ferrone CR, Mullarky E, Shyh-Chang N, et al. Glutamine supports pancreatic cancer growth through a KRAS-regulated metabolic pathway. *Nature* 2013;**496**:101–5.

18 Sousa CM, Biancur DE, Wang X, Halbrook CJ, Sherman MH, Zhang L, Kremer D, Hwang RF, Witkiewicz AK, Ying H, et al. Pancreatic stellate cells support tumour metabolism through autophagic alanine secretion. *Nature* 2016;**536**:479–83.

19 Ying H, Kimmelman AC, Lyssiotis CA, Hua S, Chu GC, Fletcher-Sananikone E, Locasale JW, Son J, Zhang H, Coloff JL, et al. Oncogenic Kras maintains pancreatic tumors through regulation of anabolic glucose metabolism. *Cell* 2012;**149**:656–70.

20 Halbrook CJ, Pontious C, Kovalenko I, Lapienyte L, Dreyer S, Lee HJ, Thurston G, Zhang Y, Lazarus J, Sajjakulnukit P, et al. Macrophage-released pyrimidines inhibit gemcitabine therapy in pancreatic cancer. *Cell Metab* 2019;**29**:1390–1399e1396.

21 Brandi J, Dando I, Pozza ED, Biondani G, Jenkins R, Elliott V, Park K, Fanelli G, Zolla L, Costello E, et al. Proteomic analysis of pancreatic cancer stem cells: Functional role of fatty acid synthesis and mevalonate pathways. *J Proteomics* 2017;**150**:310–22.

22 Zikos T, Pham K, Bowen R, Chen AM, Banerjee S, Friedland S, Dua MM, Norton JA, Poultsides GA, Visser BC, et al. Cyst fluid glucose is rapidly feasible and accurate in diagnosing mucinous pancreatic cysts. *Am J Gastroenterol* 2015;**110**:909–14.

23 Park WG, Wu M, Bowen R, Zheng M, Fitch WL, Pai RK, Wodziak D, Visser BC, Poultsides GA, Norton JA, et al. Metabolomic-derived novel cyst fluid biomarkers for pancreatic cysts: glucose and kynurenine. *Gastrointest Endosc* 2013;**78**:295–302e292.

24 Nordstrom A, Want E, Northen T, Lehtio J, Siuzdak G. Multiple ionization mass spectrometry strategy used to reveal the complexity of metabolomics. *Anal Chem* 2008;**80**:421–9.

25 Lacy P, McKay RT, Finkel M, Karnovsky A, Woehler S, Lewis MJ, Chang D, Stringer KA. Signal intensities derived from different NMR probes and parameters contribute to variations in quantification of metabolites. *PLoS One* 2014;**9**:e85732.

26 Benjamini Y, Hochberg Y. Controlling the false discovery rate: a practical and powerful approach to multiple testing. *J R Stat Soc* 1995;**57**:289–300.

27 Elta GH, Enestvedt BK, Sauer BG, Lennon AM. ACG clinical guideline: diagnosis and management of pancreatic cysts. *Am J Gastroenterol* 2018;**113**:464–79.

28 Gaiser RA, Pessia A, Ateeb Z, Davanian H, Fernandez Moro C, Alkharaan H, Healy K, Ghazi S, Arnelo U, Valente R, et al. Integrated targeted metabolomic and lipidomic analysis: a novel approach to classifying early cystic precursors to invasive pancreatic cancer. *Sci Rep* 2019;**9**:10208.

29 Morgell A, Reisz JA, Ateeb Z, Davanian H, Reinsbach SE, Halimi A, Gaiser R, Valente R, Arnelo U, Chiaro MD, et al. Metabolic characterization of plasma and cyst fluid from cystic precursors to pancreatic cancer patients reveal metabolic signatures of bacterial infection. *medRxiv* 2020.

30 Bhala A, Willi SM, Rinaldo P, Bennett MJ, Schmidt-Sommerfeld E, Hale DE. Clinical and biochemical characterization of short-chain acyl-coenzyme A dehydrogenase deficiency. *J Pediatr* 1995;**126**:910–15.

31 Shirao K, Okada S, Tajima G, Tsumura M, Hara K, Yasunaga S, Ohtsubo M, Hata I, Sakura N, Shigematsu Y, et al. Molecular pathogenesis of a novel mutation, G108D, in short-chain acyl-CoA dehydrogenase identified in subjects with short-chain acyl-CoA dehydrogenase deficiency. *Hum Genet* 2010;**127**:619–28.

32 Koeberl DD, Young SP, Gregersen NS, Vockley J, Smith WE, Benjamin DK Jr, An Y, Weavil SD, Chaing SH, Bali D, et al. Rare disorders of metabolism with elevated butyryl- and isobutyryl-carnitine detected by tandem mass spectrometry newborn screening. *Pediatr Res* 2003;**54**:219–23.

33 Chen D, Feng X, Lv Z, Xu X, Lu Y, Wu W, Wu H, Liu H, Cao L, Ye S, et al. ACADS acts as a potential methylation biomarker associated with the proliferation and metastasis of hepatocellular carcinomas. *Aging (Albany NY)* 2019;**11**:8825–44.

34 Manzo T, Prentice BM, Anderson KG, Raman A, Schalck A, Codreanu GS, Nava Lauson CB, Tiberti S, Raimondi A, Jones MA, et al. Accumulation of long-chain fatty acids in the tumor microenvironment drives dysfunction in intrapancreatic CD8+ T cells. *J Exp Med* 2020;**217**.

35 Wu L, Zhou B, Oshiro-Rapley N, Li M, Paulo JA, Webster CM, Mou F, Kacergis MC, Talkowski ME, Carr CE, et al. An ancient, unified mechanism for metformin growth inhibition in C. elegans and cancer. *Cell* 2016;**167**:1705–1718e1713.